

# Similarity Renormalization, Hamiltonian Flow Equations, and Dyson's Intermediate Representation

T.S. Walhout<sup>y</sup>

European Center for Theoretical Studies in Nuclear Physics and Related Areas  
Villa Tambosi, Strada delle Tabarelle 286; I-38050 Villazzano (Trento), Italy

## Abstract

A general framework is presented for the renormalization of Hamiltonians via a similarity transformation. Divergences in the similarity flow equations may be handled with dimensional regularization in this approach, and the resulting effective Hamiltonian is finite since states well-separated in energy are uncoupled. Specific schemes developed several years ago by Glazek and Wilson and contemporaneously by Wegner correspond to particular choices within this framework, and the relative merits of such choices are discussed from this vantage point. It is shown that a scheme for the transformation of Hamiltonians introduced by Dyson in the early 1950's also corresponds to a particular choice within the similarity renormalization framework, and it is argued that Dyson's scheme is preferable to the others for ease of computation. As an example, it is shown how a logarithmically converging potential arises simply at second order in light-front QCD within Dyson's scheme, a result found previously for other similarity renormalization schemes. Steps toward higher order and nonperturbative calculations are outlined. In particular, a set of equations analogous to Dyson-Schwinger equations is developed.

11.10.Ef; 11.10.Gh; 12.38.+t

Typeset using REVTeX

---

<sup>y</sup>email address: walhout@ect.unin.it

## I. INTRODUCTION

While particle physics has been and remains to be guided by the desire to understand phenomena at ever shorter distances, one may nevertheless argue that the most vital challenge for quantum field theory has little to do with the physics at Planck length scales or a theory of everything (TOE). This challenge is how to solve strongly interacting quantum field theories, which inevitably amounts to understanding in a nonperturbative way how a theory designed to fit the physics of a smaller scale will determine the phenomena observed at greater length scales. The prototype is Quantum Chromodynamics (QCD), but the problem has existed since soon after the development of the renormalization program for Quantum Electrodynamics, when physicists began to study strongly interacting meson theories; and the problem must presumably be confronted by anyone who wants to show that any given TOE is indeed a TOE.

In ordinary quantum mechanics, strongly interacting systems may be handled by a variety of techniques based upon a Hamiltonian formulation of the theory in question. Relativistic quantum field theory, on the other hand, is studied almost exclusively in the Lagrangian formulation nowadays. Lagrangian methods are favored because they better allow one to keep symmetries of the theory manifest. However, this generally entails a sacrifice in calculational flexibility, with the result that one is limited to applications for which perturbative or semiclassical methods are valid (or at least hoped to be valid). This paper takes the view that a Hamiltonian formulation will provide a better starting point for the study of strongly interacting quantum field theories. It was this motivation, and the difficulties in its realization, that eventually led Wilson to formulate his version of the renormalization group.<sup>1</sup>

The renormalization group is most often used in a very restricted way in quantum field theory. Typically, renormalization is used as a tool only to cover up infinities, to select out well-behaved ("renormalizable") theories, and to make finite redefinitions of couplings so as to reorganize perturbative expansions in a better way. Renormalization transformations that produce more complicated interaction terms are generally avoided. This is because such transformations usually break at least some symmetries and complicate perturbative expansions. For a theory like QCD, however, perturbation theory is not powerful enough to calculate low-energy phenomena, for the lowest orders of a perturbative expansion look nothing like what finds from low-energy experiments. In such a case, it might be worthwhile to consider a renormalization group transformation that brings new interactions, even if such a transformation hides symmetries that in the usual perturbative scheme remain manifest. The idea is that such a renormalization group transformation can be designed so that the new interactions it generates will contain the most important physics.

In fact, this is the major motivation behind the similarity transformation of Hamiltonians.<sup>2</sup> The object of the similarity transformation is not primarily to produce a renormalized Hamiltonian, but rather to produce a Hamiltonian that can be dealt with in a way such that

---

<sup>1</sup>Matrix elements of the transformed Hamiltonian  $H^0$  are "similar" to the original Hamiltonian  $H$  if  $H^0 = P H P^{-1}$ . If  $H^0$  is to be hermitian, we need  $P^\dagger = P^{-1}$ , and so the similarity transformations described here will all be unitary transformations.

even first approximations in its analysis provide a qualitatively correct description of the physics. That the similarity transformation can be used to renormalize a Hamiltonian that contains divergences is just a particular result of this more general requirement. The practical manifestation of this basic requirement is that the similarity transformation produces a Hamiltonian where only states of nearby energy contribute to phenomena at a given energy scale. Thus Glazek and Wilson<sup>2</sup> first introduced their similarity transformation to deal with divergences in light-front field theory, but also with the idea of using it to help transform the QCD Hamiltonian into a form for which a lowest-order approximation begins to look like a constituent quark model.<sup>3</sup> Wegner,<sup>4</sup> on the other hand, independently, but at roughly the same time, introduced a set of Hamiltonian flow equations to deal with many-body problems which have no need of the renormalization of divergences.

We shall follow the presentation of the similarity renormalization scheme given in Ref. [3], generalizing it in the following. The transformations of Wegner and of Glazek and Wilson will be seen to follow from more specific choices within our formalism. These three authors are generally given credit for introducing the similarity transformation to field theory. Interestingly enough, however, soon after the development of renormalization theory, Dyson himself in a difficult, fascinating, and seemingly universally ignored series of papers<sup>5</sup> developed what he called the intermediate representation, which results from a transformation that matches all the requirements of the similarity transformations developed by Glazek, Wilson, and Wegner. This is of more than just historical interest<sup>6</sup>: we shall see that Dyson's scheme has some features that lead it to be preferred over the more recent schemes.

The outline of the paper is as follows. This section has been an introduction. In the next section we provide a general interaction representation formulation of the similarity renormalization of Hamiltonians with respect to differences in unperturbed energies. We show how the schemes of Wilson and Glazek and of Wegner correspond to specific choices in our framework and argue that one might be able to make a more manageable specific choice of transformation than these. In Section III we discuss the perturbative solution of the similarity flow equations for these schemes and conclude that the corresponding diagrammatic expansion, which corresponds to that of old-fashioned time-ordered perturbation theory, leaves something to be desired in terms of computational simplicity.

This leads to a detailed discussion of Dyson's intermediate representation, which we show corresponds to a specific choice of perturbative scheme in the similarity renormalization framework. The beauty of Dyson's scheme is that it may be represented diagrammatically in terms of generalized Feynman graphs | generalized in that amplitudes may be on-energy shell. The difficulty comes in demonstrating this, and we dedicate some space to summarizing Dyson's presentation. Once the diagrammatic expansion is developed, we conclude that Dyson's scheme is much simpler computationally | at least for perturbative solutions | than those of Wilson, Glazek and Wegner. We end this long section with an example calculation taken from QCD.

In Section IV we formulate the solution of the similarity flow equations in terms of general  $n$ -particle "dressed" vertices. The resulting equations, which look much like Dyson-Schwinger equations, are of second order in these vertices; and we show how a specific choice of similarity transformation | a modification of Wegner's scheme | can guarantee that these dressed vertices are joined by Feynman propagators, which therefore permit a Wick rotation to Euclidean space. We show how analogous equations can also be derived in

Dyson's scheme and that these equations are linear in the dressed vertices. Finally, we give a specific example of how one may make approximations to sum a set of diagrams similar to those summed in the Bethe-Salpeter equation.

We shall refer to a generic theory of fermionic and vector bosonic fields throughout the paper. To provide a flavor of the type of calculation involved here, we give specific examples for QCD in light-front coordinates and light-cone gauge, but we shall only refer to other work that presents the Feynman rules for these particular calculations. In Section III, we show that the similarity-transformed Hamiltonian contains a potential that rises logarithmically for large quark-antiquark separations, a result obtained previously in other similarity renormalization schemes. In Section IV we discuss a ladder-type summation of these potentials. These examples are only meant to be suggestive. More detailed applications of our similarity renormalization framework will be undertaken in future papers.

Section V concludes the paper with a discussion of the ideas presented here. This last section is not just a summary but rather is intended to be an integral part of the paper, for it provides further motivation that could not properly be given before the scheme itself was developed. In particular, the significance of the similarity renormalization scheme for applications in light-front field theory and the motivation for the use of light-front coordinates in field theory in this light are discussed at length.

## II. SIMILARITY RENORMALIZATION SCHEME

### A. General formulation

We begin with a regularized field theoretical Hamiltonian  $H$ , derived in the usual way from a renormalizable relativistic Lagrangian. We write  $H = H_0 + H_{\text{int}}$ , with  $H_0$  the usual free Hamiltonian. Let us assume that  $H$  describes processes which at high energies may be well approximated by treating the interaction  $H_{\text{int}}$  perturbatively, but that its low-energy processes and its bound states are essentially nonperturbative. Clearly, the problem here is that  $H_0$  is a poor first approximation for calculating low-energy phenomena. The similarity renormalization scheme seeks to change the original Hamiltonian into a form that is more suitable for calculations over a wider range of energies. This is done by introducing an energy scale via a similarity transformation  $S$  (which will always be unitary here). Roughly speaking, the transformed Hamiltonian  $\tilde{H} = S H S^\dagger$  will depend on  $\mu$ , the similarity scale, as follows: processes described by  $H$  which transfer an energy much greater than  $\mu$  will be absorbed into the structure of  $\tilde{H}$ , so that  $\tilde{H}$  will only describe processes that correspond to energy transfers of order  $\mu$  or less.

Thus we call  $H$  the undressed Hamiltonian and  $\tilde{H}$  the dressed Hamiltonian. The undressed Hamiltonian is renormalized; that is, the undressed Hamiltonian is the sum of a bare regularized Hamiltonian  $H_B$  and a set of counterterms  $H_C$  that removes any dependence in physical quantities upon the regulators. The structure of these counterterms must be determined as one solves for the dressed Hamiltonian  $\tilde{H}$ . In particular, the counterterms in  $H$  ensure that  $\tilde{H}$  will remain finite as the regulators are removed. The dressed Hamiltonian  $\tilde{H}$  thus cannot produce infinities; and so the similarity transformation  $S$  is finite, provided that it avoids singularities corresponding to small energy denominators. This latter restriction shall be discussed presently.

To define such a transformation, we write the unitary operator  $S$  in terms of the anti-hermitian generator of infinitesimal similarity scale transformations  $T$ :

$$S = S \exp \left[ \frac{1}{\hbar} \int_0^1 T(s) ds \right]; \quad (1)$$

where  $S$  puts operators in order of increasing scale. Then the similarity transformation is given by the differential equation

$$\frac{dH}{ds} = [T(s); H(s)] \quad (2)$$

with the boundary condition  $H_1 = H$ . Now let the eigenstates of  $H_0$  be  $|j\rangle$ , with  $H_0 |j\rangle = E_j |j\rangle$ ; and write the matrix element of an operator  $O$  as  $O_{ij} = \langle i | O | j \rangle$ . We wish to choose  $T$  in such a way that

$$H_{ij} = f \left( \frac{E_i - E_j}{\hbar} \right) G_{ij}; \quad (3)$$

where the "similarity form factor"  $f(x)$  is a smooth function such that

$$\begin{aligned} \text{(i)} \quad & f(0) = 1; \\ \text{(ii)} \quad & f(x) \rightarrow 0 \text{ as } |x| \rightarrow \infty; \\ \text{(iii)} \quad & f(x) = f(-x); \end{aligned} \quad (4)$$

and  $G$  is a finite hermitian operator. The similarity function  $f$  has often been chosen to be a step function in previous work. However, this introduces nonanalyticities and in general should be avoided.

It is convenient to first write  $H = H_0 + H_{\text{int}}$  and transform to the interaction picture  $O_I(t) = e^{iH_0 t} O e^{-iH_0 t}$ , so that the "similarity flow" equation becomes

$$\frac{dH_I(t)}{dt} = \frac{dT_I(t)}{dt} [T_I(t); H_I(t)]; \quad (5)$$

where  $H_I(t) = e^{iH_0 t} H_{\text{int}} e^{-iH_0 t}$  and so the undressed interaction hamiltonian is  $H_I(t) = \lim_{\hbar \rightarrow 0} H_I(t)$ . After Fourier transforming, (3) and (5) become

$$H_I(\omega) = \sum_{ij} \frac{1}{2} (\omega - E_i + E_j) H_{ij} = f \left( \frac{\omega}{\hbar} \right) G_I(\omega) \quad (6)$$

and

$$\frac{dH_I(\omega)}{d\omega} = T_I(\omega) \frac{d}{d\omega} [T_I(\omega^0); H_I(\omega^0)]; \quad (7)$$

respectively. Now we are ready to construct some suitable similarity operators  $T(\omega)$ .

### B. Wilson's and Glazek's scheme

Wilson and Glazek first introduced similarity renormalization in the context of light-front Hamiltonian field theory.<sup>2</sup> Their transformation was later elaborated upon in Ref. [3]. Essentially, their choice of  $T$  gives

$$T_I(!) = \frac{d^{<}}{d^{>}} \frac{f^{<}}{f^{>}} \frac{1}{!} H_I(!); \quad (8)$$

which shall be called the WG scheme henceforth.<sup>y</sup> Note that property (4.i) of  $f$  ensures that  $T_I(!)$  is finite as  $! \rightarrow 0$ , thereby avoiding possible problems with small energy denominators. This is a great advantage of the similarity renormalization scheme. The flow equation for the choice (8) is

$$H_I(!) = f^{<} \frac{d^{<}}{d^{>}} H_I(!) + \frac{d^{<}}{d^{>}} \frac{d^{<}}{d^{>}} \frac{1}{2} \frac{d^{<}}{d^{>}} \frac{f^{<}}{f^{>}} \frac{1}{!} H_{I^0}(!^0); \quad (9)$$

The term  $d^0 H_{I^0}(!^0)$  on the righthand side means that when we express this as a pure integral equation it will contain terms of all orders in  $H_I$ . Presumably, this makes the equation rather difficult to solve.

### C. Wegner's scheme

Wegner introduced his Hamiltonian flow equation to study problems in condensed matter physics.<sup>4</sup> In the present notation, his equation is

$$\frac{dH}{d} = \frac{1}{3} [H_0; H]; H; \quad (10)$$

This is a similarity transformation with the choice  $T = [H_0; H]^{-3}$ . Actually, Wegner advocates that  $H_0$  include not just the free Hamiltonian but also the number conserving part of the undressed or even better, the dressed interacting Hamiltonian. These are certainly choices which one can (and, perhaps, should) make in any similarity scheme, although they shall not be pursued further in this work.

Wegner's flow equation can be seen as resulting from a specific choice of the similarity function  $f$  in a more general scheme. This scheme, referred to hereafter as the W scheme, results from the following choice of the infinitesimal transformation operator:

$$T_I(!) = \frac{d^{<}}{d^{>}} \frac{\ln f^{<}}{f^{>}} \frac{1}{!} H_I(!); \quad (11)$$

---

<sup>y</sup> In the referred work the argument of  $f$  was  $\frac{E_i - E_j}{E_i + E_j +}$ . It is the modification to simple energy differences used here that makes the use of the interaction picture convenient.

which gives the following similarity flow equation:

$$H_I(l) = f(l) : H_I(l) + \int_0^l d\tau \frac{d}{d\tau} \ln f(\tau) [H_I(l) ; H_I(l)^\tau] ; \quad (12)$$

This closed integralequation looks more promising than (9), although it is still nonlinear in the dressed Hamiltonian. To recover Wegner's flow equation, then, one just choses  $f(x) = e^{\frac{1}{2}x^2}$ , which fulfills all the requirements (4) of a similarity function. Using (6), the flow equation (12) becomes

$$G_I(l) = H_I(l) + \int_0^l \frac{d}{d\tau} F(\frac{1}{2}l + \tau; \frac{1}{2}l) G_I(\frac{1}{2}l + \tau; G_I(\frac{1}{2}l)^\tau) ; \quad (13)$$

where

$$F(l_1; l_2) = \frac{f(l_1) f(l_2)}{f(l_1 + l_2)} \quad (14)$$

With Wegner's choice of  $f$ , the form factor in (13) is  $F_0 = (\frac{1}{2}l + \tau)^2 e^{\frac{1}{2}\tau^2} e^{-\frac{1}{2}(l+\tau)^2}$ ; and the divergent dependence on  $l$ , while tamed by the overall factor  $f(l)$  in (12), will nevertheless favor higher orders in an iterative solution of  $H_I(l)$ .

A similarity function  $f(x)$  that falls off less sharply — for example, of the form  $(1+x^2)^{-m}$ , which goes as  $x^{-2m}$  when  $x \rightarrow 1$  — is likely to be preferred over Wegner's choice. In particular, for  $m = 1$  this latter choice gives

$$F_0(\frac{1}{2}l + \tau; \frac{1}{2}l) = \frac{(l + 2\tau)(\tau + l^2)}{(\tau + (\frac{1}{2}l + \tau)^2)(\tau + (\frac{1}{2}l + l)^2)} ; \quad (15)$$

which falls off as  $l^{-3}$  when  $l \rightarrow 1$ . This damps far-off-diagonal contributions to  $G_I(l)$  that come from the nonlinear term in (13). We shall see other reasons to prefer this choice in the following.

### III. PERTURBATIVE SOLUTION AND INTERMEDIATE REPRESENTATION

#### A. In the W G and W schemes

One may look for solutions to the similarity flow equations by expanding in the undressed interaction  $H_I(l)$  via

$$G_I(l) = \sum_{n=0}^{\infty} \frac{d!_n}{2^n} g_{1::n}^{(n)}(l) H_I(l_1) \cdots H_I(l_n) ; \quad (16)$$

Then the functions  $g_{k::n}^{(n)}(l) = g^{(n)}(l; l_k; \dots; l_n); n \geq 1$ ; satisfy the recursion equations

$$g_{1::n}^{(n)}(!) = \sum_{m=1}^n \int d^0 \left( f\left(\frac{!_m}{!_0}\right) g_{0_1::m-1}^{(m-1)}(!_m) \frac{d}{d^0} \frac{1}{!_m} f\left(\frac{!_m}{!_0}\right) g_{0_m+1::n}^{(n-m)}(!_m) \right. \\ \left. \frac{d}{d^0} \frac{1}{!_m} f\left(\frac{!_m}{!_0}\right) g_{0_1::m-1}^{(m-1)}(!_m) f\left(\frac{!_m}{!_0}\right) g_{0_m+1::n}^{(n-m)}(!_m) \right) \quad (17)$$

for the W G scheme and

$$g_{1::n}^{(n)}(!) = \sum_{m=1}^n \int d^0 \left( \frac{F_0(!_m; !_m)}{!_m} \frac{F_0(!_m; !_m)}{!_m} \right) \\ g_{0_1::m-1}^{(m-1)}(!_m) g_{0_m+1::n}^{(n-m)}(!_m) \quad (18)$$

for the W scheme, with  $g^{(0)} = 1$  for both schemes.

The similarity transformed Hamiltonian is then obtained by normal ordering the field operators in the righthand side of (16), giving a unique representation in terms of normal-ordered products of field operators:

$$G_I(!) = \sum_{m=0}^{\infty} \int d^0 \left( \frac{d^0 !_i}{2} g_{1::m}^{(m)}(!) : H_I(!_1) \dots H_I(!_m) : \right) \quad (19)$$

A given normal-ordered term with coefficient  $g^{(m)}$  in the dressed Hamiltonian will have contributions from an infinite number of terms with  $n > m$  in the expansion (16), with each contribution consisting of an integration over the product of  $g^{(n)}$  with one or more functions coming from the contractions of the field operators in (16). Since these contractions do not come from time-ordered products, one has many more contraction terms than in Feynman perturbation theory. Indeed, the resulting diagrammatic expansion<sup>3</sup> is that of old-fashioned perturbation theory. The output dressed Hamiltonian is still to be solved, of course; but now we have a variety of nonperturbative methods, such as variational techniques, that can be applied.

## B. Dyson's scheme

If the scale is large enough, then it is reasonable to solve the similarity flow equations perturbatively as above; for then only high energy processes will dress  $H_I$ , and we have assumed for our theory that the interactions governing such processes are weak. However, the proliferation of diagrams in old-fashioned perturbation theory makes the above schemes quite tedious. Even second-order calculations can be rough; and in light-front field theory, where similarity renormalization methods have been in use for several years now, little (if anything) has been accomplished at higher orders. Thus it is more than just interesting to note that Dyson long ago developed a similarity renormalization scheme which is based upon the evaluation of off-energy-shell Feynman diagrams. Since Dyson's intermediate representation was developed over several long papers, we can do it little justice here: for more details and the justification of many claims one should refer to the original work.<sup>5</sup> We shall oversimplify the presentation, change the notation, and to a certain extent alter the scheme itself, in fitting it into the present work.



Dyson considered the transformation  $O_D(t) = S_D^{-1}(t)O_I(t)S_D(t)$  of interaction representation operators to another representation induced by the unitary operator

$$S_D(t) = e^{iH_0 t} S_D e^{-iH_0 t} = T e^{i \int_{t_0}^t dt H_I(t; t_0)}; \quad (20)$$

where  $T$  is the usual time-ordering operator (acting only on the integrated times in the expansion of the exponential) and

$$H_I(t; t_0) = g(t - t_0) H_I(t_0) \quad (21)$$

describes a gradual switching on of the interaction: one requires  $g(t - t_0) \rightarrow 0$  as  $t_0 \rightarrow -\infty$  and  $g(0) = 1$ .

To be precise, Dyson introduced the function  $g$  by rescaling each occurrence of the renormalized coupling  $e_R$  in  $H_I(t_i)$ , including the counterterms, via  $e_R \rightarrow g(t - t_i)e_R$ , and included in  $H_I(t; t_0)$  terms depending on time derivatives of the  $g(t - t_i)$ . Our modification to (21) simplifies the presentation, but we should keep in mind that it is desirable to take terms of order  $(e_R)^n$  in  $H_I(t; t_0)$  to be proportional to  $g^n(t - t_0)$ , so that all terms in  $H_D$  of a given order in  $e_R$  have the same strength. The modification to our presentation needed to meet this demand is straightforward: one would have  $H_I(t; t_0) = \sum_{n=0}^{\infty} a_n g^n(t - t_0) H_I^{(n)}(t_0)$ , where  $H_I^{(n)}$  is of order  $(e_R)^n$  and the  $a_n$  are dimensionless constants.

With  $S_D$  and  $g$  chosen as above, then, low-energy processes, corresponding to large times, do not modify  $O_D(t)$ ; whereas high-energy processes do. Indeed, since the function  $g$  is dimensionless, it must introduce an energy scale, which we can write explicitly via  $g(t) \rightarrow g(t/\tau)$ . Dyson chose the form

$$g(t) = \int_0^{\infty} dG(\lambda) e^{-\lambda t} \quad (22)$$

(so  $g$  is the Laplace transform of  $G$ ) and showed that if one imposes the condition  $g^0(0) = 0$  [that is,  $\int_0^{\infty} dG(\lambda) = 0$ ] then the (Fourier-transformed) intermediate representation Hamiltonian obeys

$$H_D(\lambda) \sim \frac{1}{\lambda^2} \text{ as } \lambda \rightarrow 0; \quad (23)$$

demonstrating that  $S_D(t)$  induces a similarity transformation as defined above. Note that as  $\lambda \rightarrow 0$ ,  $g \rightarrow 1$  (which implies  $\int_0^{\infty} dG(\lambda) = 1$ ); and so in this limit  $S_D(t)$  becomes the familiar time-evolution operator that transforms from the Heisenberg to the interaction pictures. In this sense, then, for finite  $\lambda$ ,  $S_D(t)$  can be considered as transforming to an intermediate representation, which we have labelled with a  $D$  (Dyson picture) since the label  $I$  has already been taken. The intermediate Hamiltonian is

$$\begin{aligned} H_D(t) &= S_D^{-1}(t) [H_0 + H_I(t)] S_D(t) \\ &= \sum_{n=0}^{\infty} i^n \int_{t_0}^t dt_1 g(t - t_1) \int_{t_0}^{t_1} dt_2 g(t - t_2) \\ &\quad \int_{t_0}^{t_2} dt_n g(t - t_n) [H_I(t_n); \dots; H_I(t_2); H_I(t_1); H_0 + H_I(t)] \dots; \end{aligned} \quad (24)$$

and the infinitesimal similarity transformation operator associated with  $S_D(t)$  is

$$\begin{aligned} T_D(t) &= S_D^{-1}(t) \frac{d}{dt} S_D(t) \\ &= \sum_{n=1}^{\infty} \frac{i^n}{n!} \int_1^{Z^t} dt_1 \int_1^{Z^{t_1}} dt_2 \dots \int_1^{Z^{t_{n-1}}} dt_n g(t, t_1) \dots g(t, t_n) [H_I(t_n); \dots; H_I(t_2); H_I(t_1)] \dots \end{aligned} \quad (25)$$

Thus Dyson's transformation is an explicit perturbative representation of a similarity transformation, and the label  $D$  will always imply a scale dependence.

Writing  $H_D(t) = H_0 + H_I^D(t)$  and integrating by parts, we may express (24) as

$$\begin{aligned} H_I^D(t) &= \sum_{n=0}^{\infty} \frac{i^n}{n!} \int_1^{Z^t} dt_0 \int_1^{Z^{t_0}} dt_1 \dots \int_1^{Z^{t_{n-1}}} dt_n g(t, t_0) \dots g(t, t_n) [H_I(t_n); \dots; H_I(t_2); H_I(t_1); H_I(t_0)] \dots \end{aligned} \quad (26)$$

Note that for finite  $t$  the  $t$ -dependence of the intermediate Hamiltonian is still that of an interaction picture operator:  $H_I^D(t) = e^{iH_0 t} H_I^D e^{-iH_0 t}$ . Now (26) may be expressed in the alternate form

$$\begin{aligned} H_I^D(t) &= \int_1^{Z^t} dt_0 g^0(t, t_0) \\ &\quad + \sum_{m,n=0}^{\infty} \frac{i^m}{m!} \frac{i^n}{n!} \int_1^{Z^t} dt_1 \dots \int_1^{Z^{t_m}} dt_{m+n} g(t, t_1) \dots g(t, t_{m+n}) \\ &\quad \overline{T} f H_I(t_{n+1}) \dots H_I(t_{n+m}) g T f H_I(t_0) \dots H_I(t_n) g; \end{aligned} \quad (27)$$

where  $\overline{T}$  orders in the sense opposite to  $T$ . This latter form allows the normal-ordered Hamiltonian to be built up in terms of connected Feynman graphs. Let us briefly review Dyson's derivation.

First, as above, we must express the intermediate Hamiltonian in terms of a sum over normal-ordered products of field operators. For the chronologically ordered and antichronologically ordered time products (the latter results from the Hermitian conjugate of the former) we can use Wick's theorem. Field contractions from these are then the usual Feynman propagators (and their complex conjugates), and we are left with a product of two sets of normal-ordered operators. In normal ordering this remaining product, whose operators are not related chronologically, one finds field contractions that do not correspond to Feynman propagators. For example, we have

$$(x)(x^0) = : (x)(x^0) : + S_+(x, x^0); \quad (28)$$

$$D_+(\mathbf{x}, \mathbf{x}^0) = \int_{\mathbf{x}^0}^{\mathbf{x}} \mathbf{f}_B e^{-i\mathbf{k} \cdot (\mathbf{x} - \mathbf{x}^0)} d\mathbf{x}; \quad (29)$$

$$dk_B = \frac{d^4 k}{(2\pi)^3} \delta(k_0) \delta(k^2 - m_B^2) \quad (31)$$

$$H_I^D(!) = \sum_{m,n=0}^{\infty} \frac{x^1}{m!} \frac{(-i)^n}{n!} : \prod_{i=0}^{8-m-n-1} d_i G(-i); \prod_{fpg}^9 = X M_{mn}^{fpg}(!; ) N_{fpg}^{FFB}; \quad (32)$$
$$N_{\text{fpg}}^{\text{FFB}} = : y(p_1) \cdots y(p_F) y(p_{F+1}) \cdots y(p_{F+F_A}) y(p_{F+F_A+1}) \cdots y(p_{F+F_A+F_B}) :; \quad (34)$$

$$X_{\text{fpg}}^M \overset{\text{fpg}}{M}_{mn} N_{\text{fpg}} = \int_{i=0}^8 dt_i \int_{j=0}^9 dt_j e^{i(\dots)} (t_i, t_j) \quad (36)$$

11

that these abnormal contractions will contribute Fourier components  $e^{ik_1 \cdot (\sum x_j)}$  with the zeroth component  $k_1^0 = 0$ : We have then  $k_1^0 = m$  in  $(m_B; m_F)$  for all L abnormal contractions.

Next we make the shift of integration variables  $t_j \rightarrow t_j + t$  for  $j \leq n$  and consider  $M_{m,n}^{fpg}$  as a function of the variables  $\epsilon_i$  and  $m_{B,F}$ . In calculating  $M$ , we consider the  $\epsilon_i$  to be pure imaginary numbers in order to perform the time integrations, which have been extended to positive infinity. After these changes, the integration over  $t$  in (36) yields a delta-function

$$M_{m,n}^{fpg}(\epsilon; ) / \left( \prod_{i=n+1}^L \epsilon_i^{m} \prod_{j=0}^n \epsilon_j^{n} \prod_{l=1}^N k_l^0 \right); \quad (37)$$

where  $\epsilon_j$  is the algebraic sum of the zeroth components of the external momenta  $p_k$  that meet vertex  $j$ , so that  $\epsilon = \prod_{k=1}^F p_k^0$ ,  $F + F + B$ ,  $p_k^0 = \prod_{i=0}^{m_F+n} \epsilon_i$ . If we assume that  $m_B$  and  $m_F$  are large enough, then

$$\prod_{l=1}^L k_l^0 = L \text{ in } (m_B; m_F) > \prod_{i=n+1}^L \epsilon_i^m \prod_{j=0}^n \epsilon_j^n \quad (38)$$

so that (37) cannot be satisfied and  $M_{m,n}^{fpg}$  vanishes for  $m \geq 1$ . Thus for  $\text{Re}(\epsilon_i) = 0$  and  $m_{B,F}$  satisfying (38),  $M$  may be found from (36) with  $m = 0$ , which then is simply an on-energy-shell Feynman amplitude. Dyson argued that considered as a complex function of the variables  $m_{B,F}$  and  $\epsilon_i$ ,  $M$  is analytic, and thus this representation of  $M$  is unique. So to obtain the intermediate Hamiltonian, one need simply calculate  $M$  with the variables constrained as above (so that one can use generalized Feynman graphs), then analytically continue first  $m_{B,F}$  from large values down to their physical values and then the  $\epsilon_i$  from pure imaginary back to pure real numbers (in practice, this analytic continuation is trivial). Finally, the integrals over the  $\epsilon_i$  in (32) may be performed.

### C. Doubled Feynman graphs and spurions

Dyson described a graphical method,<sup>y</sup> using what he called "doubled" Feynman diagrams, for calculating intermediate representation operators from expressions such as (36). A doubled Feynman diagram is an ordinary connected  $n+1$ -point Feynman graph in which a simply connected "tree" of (fermion and/or boson) propagator lines are drawn double. An example is given in Figure 1. The doubled lines account for the factors  $e^{-it_i}$  that occur at each point  $x_i$  and spoil energy conservation. If it is possible to draw more than one doubled Feynman graph from a given Feynman graph, one of these is chosen arbitrarily and the rest are ignored (they are not distinct, each one being obtained from any other by a suitable change in the internal momentum variables). Dyson then describes in detail how to shift the momenta of the doubled propagators consistently to account for the dependence of  $M$  upon the  $\epsilon_i$ . The rules are somewhat involved.

<sup>y</sup>Although, sadly, his papers have no figures.

$$(\mathbf{t} - \mathbf{t}_0) = \frac{Z}{2i} \frac{e^{i(\mathbf{t} - \mathbf{t}_0)}}{j''} = \frac{Z}{2i} \frac{e^{i(\mathbf{t} - \mathbf{t}_0)}}{j''}; \quad (39)$$
$$\int_{\text{fpg}} \prod_{m,n} d^4 x_m d^4 x_n = \int_{m=0}^Z \frac{d i_0}{2} \int_{i''}^Z dt e^{i(\dots)} \dots \quad (40)$$
$$P_I^D(p) = n H_I^D(p) = \sum_{n=0}^{\infty} \frac{x^n}{n!} \sum_{i=0}^{\infty} d_i G(i) \frac{d}{2} \frac{i_0}{i''} \quad (41)$$
$$M_n^{\text{fpg}}(\mathbf{p}; \mathbf{f}, \mathbf{g};) = (2)^4 \cdot (4) (\mathbf{p} \cdot \mathbf{p}^0 + \mathbf{p}^{\text{I}}) M_n^{\text{fpg}}(\mathbf{f}, \mathbf{g};): \quad (42)$$
$$(2)^4 (4) (p_i^0 \quad \bar{p} + q_i^0 \quad \bar{q} \quad (i_{-i} + i_0) ) \quad (43)$$

The amplitudes  $M_n^{\text{fpg}}$  are connected  $n + 1$ -point Feynman diagrams whose dependence upon  $\epsilon$  and the  $\epsilon$  may be accounted for by drawing an additional directed dashed line as in Figure 2, which is equivalent to Figure 1. This is very similar to the spurion line of Kadyshchewsky's diagrammatic scheme.<sup>7</sup> Although the rules for our scheme are quite different than those of Kadyshchewsky's, we shall still call our dashed line a spurion line. We treat the

variables  $k_i = p_i - \sum_{j=0}^i p_j$  as momenta and stipulate that the spurion line carries momentum as shown in Figure 2 | namely, the spurion line entering vertex  $i$  has momentum  $k_i$ , and that exiting vertex 0 has momentum  $k_0$ . The spurion line touches each vertex exactly once, proceeding in decreasing order from vertex  $n$  to 0. A relabeling of the vertices 1 through  $n$  will not produce a distinct diagram since (41) is symmetric with respect to  $i \leftrightarrow j, i \neq j \neq 0$ , and so for a given choice of vertex 0 we may choose any ordering of 1 through  $n$  and ignore all others, for they just sum to cancel the factor  $\frac{1}{n!}$  in (41). We may think of the spurion line as ordering the different vertices in time; however, it is only the order of vertex 0 that need be distinguished from that of the others.

With the spurion line considered as carrying momentum in the way described above, we have the usual four-momentum conservation at each vertex; and the evaluation of the amplitude  $M$  proceeds as that of an ordinary Feynman graph. The spurion line serves only to shift the internal momenta so that the dependence on the  $k_i$  is now carried by the Feynman propagators | this is precisely the role of the doubled lines in Dyson's formulation. There will also always be an overall  $\delta$ -function of the form  $\delta^{(4)}(p_n + \dots)$ , which expresses conservation of total three-momentum but not energy. The dependence of  $M$  upon the variables  $k_0$  and  $k_n$  comes solely from this latter  $\delta$ -function, and so the integrals over these variables in (41) will yield the similarity function described earlier, a function that by choice of  $G(k_0)$  falls off at least as rapidly as  $\frac{1}{k_0^2}$  when the total energy difference  $k_0 = p_0$  diverges.

The most obvious advantage of Dyson's scheme is the apparent invariance of the expression (41). The  $k_i$  and  $k_n$  are dimensionless scalars, and covariance is broken only by  $\eta = \eta_n$ , which was chosen to have a special form. We note now that the choice  $\eta = (1; 0; 0; 0)$  above gives the equal-time formulation described here, but one could just as well choose  $\eta = \eta_+$  with  $\eta_+^2 = 0, \eta_+ \cdot x = x^0 + x^3$ . This latter choice of  $\eta$  ensures that (41) yields the light-front formulation of the Hamiltonian, with  $x^+$  the "light-front time." It is important, however, that divergences arising from the integrations in (41) are independent of  $\eta$ , for they occur when the internal momenta of our Feynman graphs diverge with respect to the variables  $k_i$ . Thus the determination of the counterterm structure of  $H_I$  is entirely equivalent to ordinary Feynman perturbation theory.<sup>7</sup> In particular, the usual rules for power counting, separation of divergences and multiplicative renormalizability apply, results that are by no means clear in other schemes for light-front variables.

## D. An example

As an example we shall look at the quark-antiquark potential in light-front QCD. We do not discuss at length any of the many interesting, enticing and puzzling features of light-front QCD. For more details see Ref. [3] and the many references listed therein. Here we shall only outline the calculation and give the results. When formulated using light-front

---

<sup>7</sup>As with Feynman perturbation theory, the light-cone gauge choice  $A^+ = \eta_+, A = 0$  is noncovariant and necessitates the introduction of counterterms that depend on  $\eta = (1; 0; 0; 1)$ . Such counterterms, of course, cannot depend on  $\eta$ .

variables<sup>z</sup> and light-cone gauge, half the degrees of freedom of QCD are constrained and one may develop an effective theory in which the gluons and quarks are two-component fields.<sup>9</sup> For some calculations it is more appropriate to use the original four-component constrained theory<sup>10,11</sup> — for example, to demonstrate that the Slavnov-Taylor identities are fulfilled.<sup>12,11</sup> In general, however, calculations are much easier in the two-component theory, and we use just this theory here. The Feynman rules for the two-component effective theory are given in the appendix of Ref. [9]. We calculate the coefficient of the term  $N_{fpg}^{220} = : \bar{\psi}(p_3) \gamma(p_2) \gamma(p_4) \psi(p_1) :$  in the intermediate Hamiltonian to second order in the undressed coupling  $g_R$ . Perry<sup>13</sup> first showed using a discrete similarity transformation (with the similarity function  $f$  chosen to be a step function) that one obtains a logarithmically confining potential in the dressed Hamiltonian. Zhang<sup>14</sup> later showed that a continuous similarity transformation such as those described here (specifically, the WG scheme of Ref. [3] with  $f$  a step function) yields a potential of the same form. Wilson and Robertson<sup>15</sup> gave general arguments (and caveats) for the appearance of such a confining potential in similarity transformed light-front QCD Hamiltonians. Here, we show how such a potential arises within Dyson's scheme.

The graphs that contribute at second order are shown in Figure 3. Graph 3a comes from a term  $H_I^{(2)}(x)$  in the bare Hamiltonian that arises from eliminating the constrained components of the gluon field.<sup>9</sup> This term is proportional to  $(g_R)^2$ , and in the spirit of our prior discussion, we take the term  $H_I^{(2)}(x; x^0)$  appearing in the definition (20) of  $S_D$  to be proportional to  $g^2(\delta(x^0))$ . The change to our momentum space Feynman rules caused by this modification is slight: we need only alter the way the spurion line carries the momenta. If each vertex  $i$  in a given  $n+1$ -vertex diagram corresponds to a term in the Hamiltonian proportional to  $(g_R)^{m_i}$ , then we have  $m = \sum_{i=0}^n m_i$  factors  $\delta_{ij}, 1 \leq j \leq m_i$ , corresponding to the functions  $g^{m_i}(\delta_{ij}(x_{ij}))$ . Then the diagrams are exactly the same, except for the redefinition  $\delta_{ij} = \delta_{ij} \prod_{j=0}^i \prod_{k=1}^{m_j} \delta_{jk}$ . The integration in (41) is now over

$$\int \prod_{i=0}^n \prod_{j=1}^{m_i} d_{ij} G(\delta_{ij}); \quad \int \frac{d^4 m_{01}}{2i(m_{01}^2)}; \quad (44)$$

The amplitudes corresponding to the graphs in Figure 3 are thus

$$iM_a = 4ig_s^2 T^a T^a \frac{1}{p_1^+ p_3^+ p_2^+} (2)^4 \delta^{(4)}(p_0 + p_1); \quad (45)$$

where  $p = p_3 + p_4 = p_2 + p_1$  and  $p_0 = p_1 (p_1^+ + p_2^+)$ ;

---

<sup>z</sup>Light-front longitudinal momentum is  $p^+ = n_+ \cdot p = p_0 + p^3$ , light-front energy is  $p^- = n_- \cdot p = p^0 - p^3$ , and transverse momentum is  $p_\perp^i = p^i, i = 1, 2$ . The scalar product is  $p \cdot x = \frac{1}{2} p^+ x^- + \frac{1}{2} p^- x^+ + p_\perp \cdot x_\perp$ , where the notation  $p_\perp \cdot x_\perp$  means  $p^1 x^1 + p^2 x^2$ . Occasionally, it is convenient to define the light-front 3-vector  $p = (p^+, p_\perp)$  and the product  $p \cdot x = p^+ x^- + p_\perp \cdot x_\perp$ . On-shell particles satisfy  $p^2 = \frac{p_\perp^2 + m^2}{p^+}$ , from which it follows that transverse momenta scale as masses but longitudinal momenta scale differently.

$$iM_b = \left( \frac{q_2^i}{[q^+]^2} - \frac{p_3 \cdot p_1}{2[p_3^+]^2} - \frac{i}{2} \frac{p_3 + p_1}{2[p_1^+]^2} \right) \frac{4ig_s^2 T^a T^a}{q^2 + i''} \quad (46)$$

$$\left( \frac{q_2^i}{[q^+]^2} - \frac{p_3 \cdot p_2}{2[p_2^+]^2} - \frac{i}{2} \frac{p_3 + p_2}{2[p_4^+]^2} \right) (2)^4 (4) (p_{-1} + \dots);$$

where  $p$  is as above,  $p_0 = i_{01}$ ,  $p_1 = i_{11} + p_0$ , and  $q = p_3 - p + p_0 - p_1$ ; and, finally,  $M_c$  is obtained from  $M_b$  by the substitutions  $p_1 \rightarrow p_2$ , and  $p_0 \rightarrow p_1$ . In general, we need to regulate the singularities as the longitudinal momentum  $q^+ = n - q \rightarrow 0$ . As is usual for Feynman diagrams in light-front variables, we use the Mandelstam-Leibbrandt prescription<sup>16</sup>

$$\frac{1}{[q^+]} = \frac{q}{q^+ q + i''} = \frac{1}{q^+ + i'' \epsilon(q)}; \quad (47)$$

For the four-point interaction of (45), we interpret this prescription to be

$$\frac{2}{[p_1^+][p_3^+]} \rightarrow \frac{p_1 \cdot p_3}{(p_1^+)(p_3^+) + i''} + \frac{p_4 \cdot p_2}{(p_1^+)(p_3^+)(p_4^+)(p_2^+) + i''}; \quad (48)$$

The potential  $V(p_1; p_2; p_3; p_4)$  is proportional to the sum of these terms,  $M_a + M_b + M_c$  integrated over the variables  $i_j$ . We are interested in how this potential behaves at large separations, for which the terms proportional to  $[q^+]^{-1}$  will dominate the expressions in the brackets in (46). Summing the three diagrams and relabelling the  $i$ , we have then for the long-range part of the potential

$$iV_{LR}^{(3)}(p) = 4g_s^2 T^a T^a \int \frac{d^2 q}{p \cdot i(q_0 + p_1)} \quad (49)$$

$$\left( \frac{(q)^2}{(q^+ q + i'')^2} - \frac{q^+ q}{q^+ q + i''} + \frac{(q)^2}{(q^+ q + i'')^2} - \frac{q^+ q}{q^+ q + i''} \right);$$

where  $q = p_3 - p - i_1$  and  $q = p_2 - p + i_1$ . For small  $q = p_3 - p = p_2 - p$ , the energy difference  $p$  can be ignored with respect to  $i_1$ . We calculate  $V_{LR}(x; x')$ , the Fourier transform with respect to  $q$  of (49) above under this approximation. We need to be careful, however, for  $V_{LR}(0; 0)$  diverges. This is a result of well-known infrared singularities due to the choice of light-cone gauge, singularities that are known to cancel (in perturbation theory, at least) when evaluating gauge invariant quantities.

Now, when using light-front variables, we need to take into account that transverse and longitudinal variables scale differently. Thus there is a transverse mass scale  $\mu$  and a longitudinal momentum scale  $\lambda$ . The energy scale is then  $E = \mu^2 = \lambda^2$ . It is natural to use dimensional regularization to handle both ultraviolet and infrared divergences in our scheme by taking the number of transverse dimensions to be  $d$  instead of 2. Then we must introduce an arbitrary (transverse) mass scale, which we take to be  $\mu$ . This means the similarity now is governed by the longitudinal scale  $\lambda$ . That the couplings now run with two scales will have profound implications at higher orders, but this does not concern us at present. Setting  $p \rightarrow 0$  in (49), generalizing to  $d$  transverse dimensions and taking the Fourier transform, we find





can express the dressed Hamiltonian from the outset in terms of normal-ordered products of field operators as follows:

$$H_I(t) = \sum_{fpg} h_I^N(p_1; \dots; p_{F+F+B}) e^{ip_0 t} N_{FFB} \sum_{fpg} h_I^{fpg} N_{fpg}(t); \quad (54)$$

where  $p = p^0 \dots p^I$ , as before, and  $h_I^{fpg} = h_I^{fpg}(2)^3 (3) (p) \mid$  that is, total 3-momentum is conserved. Taking the Fourier transform of (12) we only consider the W scheme here we find

$$H_I(t) = \int dt^0 f(t^0) H_I(t^0) + \int d^0 \int dt^0 dt^0 f^0(t^0; t^0) H_I(t^0) H_I(t^0); \quad (55)$$

where  $f(t)$  is the Fourier transform of  $f(!)$  and

$$f^0(t_1; t_2) = \frac{d!}{2} \frac{d!^0}{2} e^{i! t_1} e^{i!^0 t_2} \frac{f(\frac{!}{!_0})}{f(\frac{!}{!_0})} \left( \frac{d \circ \ln f(\frac{!}{!_0})}{!^0} - \frac{d \circ \ln f(\frac{!}{!_0})}{!^0} \right) \quad (56)$$

Now let us choose the similarity function motivated earlier, namely,  $f(x) = (1+x^2)^{-1}$ . Then the term in the brackets in (56) has a pole structure in  $!^0$  that yields step functions in  $t_2$  after integration. We find

$$H_I(t) = \frac{1}{2} \int dt^0 e^{-it^0} H_I(t^0) + \frac{i}{4} \int d^0 \frac{1}{\omega} \int dt^0 dt^0 e^{-it^0} e^{-it^0} \left( e^{-it^0} + e^{-it^0} \right) \frac{1}{T} f H_I(t^0) H_I(t^0) g - \frac{1}{T} f H_I(t^0) H_I(t^0) g; \quad (57)$$

This is a very happy form. Indeed, when we substitute the expansion (54) in (57), we find that contractions of field operators resulting from normal-ordering the righthand side will only be of the Feynman type. Moreover, we need only consider the operator

$$K(t) = \frac{1}{4} \int dt^0 e^{-it^0} H_I(t^0) + \frac{i}{4} \int d^0 \frac{1}{\omega} \int dt^0 dt^0 e^{-it^0} e^{-it^0} \left( e^{-it^0} + e^{-it^0} \right) \frac{1}{T} f H_I(t^0) H_I(t^0) g; \quad (58)$$

since from the Hermiticity of  $H_I$  we have

$$H_I(t) = K(t) + K^\dagger(t); \quad (59)$$

The calculation of  $K$  involves only proper Feynman propagators, and one need only consider connected graphs since disconnected graphs will not contribute to  $H_I$  (they are cancelled by identical terms from  $K^\dagger$ ).

We expand  $K(t)$  as we did for  $H_I(t)$  in (54) so that  $h_I^{fpg} = k^{fpg} + (k^{fpg})^\dagger$ , where  $k^{fpg} = k(p_{F+F}; \dots; p_1; p_{F+F+B}; \dots; p_{F+F+1}) \mid$  and substitute in (58). The amplitudes  $k^{fpg}$  so defined are to be solved by iteration. One can always organize such an iterative solution to reproduce the perturbative expansion of Section III, should one care to. Indeed, by expanding the dressed amplitudes  $h_I^{fpg}$  in powers of the undressed amplitudes  $h_I^{fpg}$ , one

recovers the perturbative scheme of Section III A. However, now there are other more interesting possibilities, for just as with Dyson-Schwinger equations one can use a variety of approximations to (58) in order to sum up infinite classes of diagrams. We note that (58) permits a Wick rotation to Euclidean space and thus the normal power counting applies in determining the counterterm structure. This does not seem to be true for all choices of the similarity function  $f$ .

### B. In the Dyson picture

We can also develop Dyson-Schwinger-like equations for the intermediate Hamiltonian by introducing a new time scale  $T > 0$  into the integrals in (20). We define

$$S^D(t; T) = T e^{i \int_{t-T}^t dt^0 H_I(t; t^0)}; \quad (60)$$

so that

$$\begin{aligned} H_I^D(t; T) &= \sum_{n=0}^{\infty} \int_{t-T}^t dt_0 g^0(t-t_0) \int_{t-T}^t dt_1 g(t-t_1) \\ &\quad \int_{t-T}^t dt_n g(t-t_n) [H_I(t_n); \dots; [H_I(t_1); H_I(t_0)]] \\ &= \int_{t-T}^t dt_0 g^0(t-t_0) H_I(t_0) + i \int_{t-T}^t dt_1 g(t-t_1) [H_I(t_1); H_I^D(t; t-t_1)]; \end{aligned} \quad (61)$$

which is a linear integral equation. The usual intermediate Hamiltonian is then obtained from  $H_I^D(t; T)$  by taking the limit  $T \rightarrow 1$ .  $H_I^D(t; T)$  depends on  $t$  as an interaction representation operator — namely,  $H_I^D(t; T) = e^{iH_0 t} H_I^D(0; T) e^{-iH_0 t}$  — so we expand  $H_I^D(t; T)$  in terms of normal-ordered products of field operators each at time  $t$ , with coefficients that depend on the positions of these operators and  $T$ :

$$H_I^D(t; T) = \sum_{fpg} h_{ID}^{fpg}(T) N_{fpg}(t); \quad (62)$$

$N_{fpg}(t)$  can be expressed as a normal-ordered product of field operators such as  $\phi_i(t) e^{ip_i t}$ .  $K_D(t; T)$  is defined analogously to  $K(t)$  above, and we find

$$\begin{aligned} \sum_{fpg} h_D^{fpg}(T) N_{fpg}(t) &= \int_0^T dt^0 \int dt^1 g(t-t^0) e^{-it^0} \frac{1}{2} \sum_p h_I^{fpg} N_{fpg}(t-t^0) \\ &\quad + i \sum_{fpg; fpg^0} h_I^{fpg} h_{ID}^{fpg^0}(t^0) T \sum_n N_{fpg}(t-t^0) N_{fpg^0}(t)^3; \end{aligned} \quad (63)$$

The time-ordered product is expanded using Wick's Theorem in momentum space — for example,

$$T \prod_q(t) \prod_{q^0}(\bar{t}^0) = : \prod_q(t) \prod_{q^0}(\bar{t}^0) : + i(2)^4 (4) (q_1 \dots q_4) S_F(q) e^{i q_0(t - \bar{t}^0)} : \quad (64)$$

We represent the product of all contractions | that is, the product of  $B_q$  boson propagators  $D_F(q_i)$ ,  $F_q$   $\gamma$  propagators  $S_F(q_j)$  and  $F_q$   $\gamma$  propagators  $S_F(q_k)$  as  $M_{fpg}$ , so that we have

$$T \prod_{fpg}(t) \prod_{fpg^0}(\bar{t}^0) = \prod_{q, N_{q^0}} \prod_{B_q F_q F_q}^{8} (2)^4 (4) (q_1^0 \dots q_4^0); \quad (65)$$

$$M_{fpg} : N_{fp=qg}(t) N_{fp^0=q^0g}(\bar{t}^0) : e^{i p^0(t - \bar{t}^0)} :$$

The notation  $N_{fp=qg}$  means the  $N_q = F_q + F_q + B_q$  field operators with  $p_i = q_i$  (those corresponding to the contractions) are dropped from the normal-ordered product  $N_{fpg}$ . Expressing the amplitudes as

$$k_D^{fpg}(T) = \int_0^T dt \frac{1}{1 + i p^0} e^{(1 + i p^0)T} R_D^{fpg}(t) \quad (66)$$

and similarly for  $h_{ID}^{fpg}(T)$ , after a bit of manipulation (63) becomes

$$R_D^{fpg}(t) = \frac{1}{2} G(t) h_I^{fpg} + i \int_0^t dt' G(t-t') \prod_{fpg F_p^0 F_p^0 B_p^0} X \frac{h_I^{fp^0 qg} M_{fpg} R_{ID}^{fp=p^0 qg}(t-t'; p^0, q)}{(t-t') + i(p^0 - p^0 - q)} : \quad (67)$$

This equation has a simple graphical interpretation in analogy with the spurion diagrams of Section III C. If we define the dressed amplitudes  $k_D^{fpg}(t; p, q) = 2(t - i) R_D^{fpg}(t; p, q)$  and  $h_{ID}^{fpg}(t; p, q) = 2(t - i) h_{ID}^{fpg}(t; p, q)$  and the undressed amplitude  $h_I^{fpg}(t; p, q) = 2(t - i) G(t) h_I^{fpg}$ , then (67) becomes

$$k_D^{fpg}(t; p, q) = \frac{1}{2} h_I^{fpg}(t; p, q) + \int_0^t dt' \frac{1}{2} \prod_{fpg F_p^0 F_p^0 B_p^0} X \frac{h_I^{fp^0 qg}(t-t'; p, q) M_{fpg} h_{ID}^{fp=p^0 qg}(t-t'; p, q)}{(t-t') + i(p^0 - p^0 - q)} : \quad (68)$$

If we draw a spurion line as in Figure 4, entering the undressed vertex with momentum  $i$ , carrying momentum  $(p^0 + i, i^0)$  from the undressed to the dressed vertex and exiting the last vertex with momentum  $q$ , then the total 4-momentum is conserved at each vertex.

Figure 4 is a graphical representation of (68) for the  $N_{fpg}^{220}$  amplitude. Undressed vertices are denoted by a dot, and dressed vertices (of type  $k_D$  or  $h_D$ ) are denoted by a bubble. The resemblance to Dyson-Schwinger equations is evident. The dots indicate that we have not shown diagrams that modify the quark legs only (counterterm diagrams from the undressed Hamiltonian and  $\gamma$ -dependent mass terms from the dressed Hamiltonian) as well as diagrams that involve dressed vertices with more than five total quark and gluon legs. The diagrams for  $k_D^\gamma$  are equivalent to those shown here, except the direction of the spurion line is reversed. Diagrammatically, it is easy to see how an iterative solution of these equations, starting with the undressed vertices as input, will reproduce the perturbative diagrams of Section

III.C. Of course, the diagrams are precisely equivalent only in the limit  $T \rightarrow 1$ . Note that because the amplitude  $k_D(p_3; p_2; p_1; p_1)$  enters  $K_D$  as the coefficient of  $N^{220}(p_3; p_2; p_1; p_1)$ , which is antisymmetric under either  $p_1 \leftrightarrow p_2$  or  $p_3 \leftrightarrow p_2$  and symmetric under  $(p_1; p_2) \leftrightarrow (p_3; p_2)$  plus complex conjugation, the diagrams in Fig. 4 represent additional processes — for example, the last diagram shown represents processes where the undressed  $q\bar{q} \rightarrow q$  vertex is attached to any of the four quark legs.

The advantage of having an equation that is linear in the dressed vertices, as in the present case, is that the undressed Hamiltonian has a finite number of terms, whereas the dressed Hamiltonian can have terms with any number of legs. Thus a diagrammatic expansion for any given dressed vertex based upon (58), which is nonlinear in the dressed vertices, will contain an infinite number of graphs since there can be any number of internal lines connecting the two dressed vertices. In contrast, the diagrammatic expansion for any given dressed vertex based upon (68) contains a finite number of graphs, since the number of internal lines is limited by the undressed vertices.

### C. Another example

As an example of this new formulation of the similarity transformation, let us set up the calculation of an approximation to the general quark-antiquark potential in light-front QCD. We start from the diagrams in Fig. 4. There will be similar diagrammatic equations for the dressed  $q\bar{q} \rightarrow q$  and  $q\bar{q} \rightarrow q\bar{q}$  that appear in the equation for the dressed  $q\bar{q} \rightarrow q\bar{q}$  amplitude. We may approximate these latter equations as shown in Fig. 5. According to this approximation, we treat perturbatively vertices that change gluon number; in first approximation the dressed  $q \rightarrow q\bar{q}$  is equivalent to the undressed vertex. Consistent with this approximation, we take the amplitude  $q\bar{q} \rightarrow q\bar{q}$  to be as in Fig. 5. This corresponds to taking the input potential for the dressed  $q\bar{q} \rightarrow q\bar{q}$  amplitude to be as in Fig. 6. This yields the  $O(g_R^2)$  potential calculated in Section III.D. (For simplicity, we have neglected to draw the spurion lines in Figs. 5 and 6.) The equation for the dressed  $q\bar{q} \rightarrow q\bar{q}$  vertex in this approximation is shown in Fig. 7. This looks very much like the Bethe-Salpeter equation. Here again, we have ignored corrections to the external legs. Clearly, improving the approximations for the gluon-number-changing vertices corresponds to including higher order radiative corrections to the input potential of Fig. 6.

While we shall not solve for this dressed amplitude here, it is perhaps instructive to set up the equations in some detail. From the above, the dressed vertices satisfy

$$\begin{aligned} h_{ID}^{fpg}(t) &= e^{ip^0 t} \lim_{T \rightarrow 1} \int_0^T d\tau \int_0^T \frac{d}{d\tau} \frac{1}{2i} \frac{e^{i\tau T}}{i''} h_{ID}^{fpg}(\tau; \tau) \\ &= e^{ip^0 t} \int_0^T d\tau \int_0^T \frac{d}{d\tau} \frac{1}{2} e^{-i\tau t} h_{ID}^{fpg}(\tau; \tau); \end{aligned} \quad (69)$$

with

$$h_{ID}^{fpg}(\tau; \tau) = h_I^{fpg}(\tau; \tau) + \int_0^T d\tau' \int_0^T \frac{d}{d\tau'} \frac{1}{2} \frac{0 \times \times}{f_{q\bar{q}} f_F^0 f_F^0 f_B^0} \quad (70)$$

$$\begin{aligned} & \frac{1}{i_0''} h_I^{fp^0 \bar{q}g} (0; 0) M_{fqq} h_{ID}^{fp=p^0 \bar{q}g} (0; 0) \\ & \frac{1}{i_0''} h_{ID}^{fp^0 \bar{q}g} (0; 0) M_{fqq} h_I^{fp=p^0 \bar{q}g} (0; 0) : \end{aligned}$$

To ease our notational burden, let us call the dressed  $qq \rightarrow qq$  vertex  $h_{ID}^{220}$ ; the dressed  $q \rightarrow qg$  vertex  $h_{ID}^{111}$ ; and the dressed  $qqg \rightarrow qq$  vertex  $h_{ID}^{221}$ . Undressed vertices will be denoted by the subscript 0 | note that  $i_0 = 0$ : Now the approximations of Fig. 5 are

$$(i; j) = i_0(j; j); \quad (71)$$

$$\begin{aligned} (i; j) &= i_0 \int \frac{d^4 q}{(2\pi)^4} \frac{1}{i_0''} (0; 0) S_F(q) (0; 0) \\ &+ \frac{1}{i_0''} (0; 0) S_F(q) i_0 (0; 0) : \end{aligned} \quad (72)$$

The undressed quark-gluon vertex is<sup>9</sup>

$$\begin{aligned} i_0(i; j) &= G(0) i_0 (2\pi)^4 (4) (p_3^0 p_1^0 q (i_1 + j_1)) \\ i_0(p_3; p_1; q) &= g T^a \frac{q_i}{[q^+]} \frac{p_3^- p_1^- \text{im}_F}{[p_3^+]} \frac{i_1^- j_1^- \text{im}_F}{[p_1^+]} : \end{aligned} \quad (73)$$

The undressed  $qq \rightarrow qq$  vertex is

$$\begin{aligned} i_0(i; j) &= \int d_0 G(0) d_1 G(1) (0_0 1_0) i_0 (2\pi)^4 (4) (p^0 (i_1 + j_1)) \\ i_0(p_3; p_2; p_1; p_1) &= 4g_R^2 T^a T^a \frac{1}{[p_3^+ p_1^+]^2} : \end{aligned} \quad (74)$$

We have seen these undressed vertices in the perturbative calculation of Sec. III D.

The next to the last graph in Fig. 4 is

$$\int d_0 \int \frac{d^4 q}{(2\pi)^4} \frac{1}{i_0''} i_0^Y(0; 0) iD(q) (0; 0) : \quad (75)$$

Using the approximation (71), this becomes

$$\begin{aligned} i_0^a(i; j) &= \int d_0 G(0) d_1 G(1) (0_0 1_0) \int \frac{d^4 q}{(2\pi)^4} \frac{1}{i_0''} \\ & i_0^Y(p_3; p_2; q) D(q) i_0(p_3; p_1; q) (2\pi)^4 (4) (p^0 (i_1 + j_1)); \end{aligned} \quad (76)$$

where  $q = p_2 - p_1 + (i_1 + j_1)$ . There is a similar contribution to  $i_0^b$  from the term  $k_{ID}^Y$ . Indeed, it is identical after the replacement  $q \rightarrow q = p_3 - p_1 - (i_1 + j_1)$  | this corresponds to reversing the direction of the spurion line. We write this as  $i_0^b = i_0^a \frac{1}{4!} q$ . After integration over  $q$ , the sum of these terms and the undressed vertex  $i_0$  gives the input potential of Fig. 6, namely:

$$\begin{aligned} V(i; j) &= \int d_0 G(0) d_1 G(1) (0_0 1_0) \int \frac{d^4 q}{(2\pi)^4} \frac{1}{i_0''} \\ &= \int d_0 G(0) d_1 G(1) i_0 (0_0 1_0) \\ & \quad \overline{V}_{fpg}(i_1 + j_1) (2\pi)^4 (4) (p^0 (i_1 + j_1)); \end{aligned} \quad (77)$$

where

$$\overline{V}_{\text{fpg}}(+i_1) = \int_0^1 (q) + \int_0^1 (q) \int_0^1 (p_2; p_1; q) D(q) \int_0^1 (p_3; p_1; q) \int_0^1 (p_2; p_1; q) D(q) \int_0^1 (p_3; p_1; q); \quad (78)$$

with  $q = p_2 - p_1 + (+i_1)$  and  $q = p_3 - p_1 - (+i_1)$ . Substituting this into (69), we recover the order  $g_R^2$  potential of Sec. IIID, as indeed we must. Thus the first and fourth terms on the righthand side of the equation in Fig. 4 (plus their conjugate graphs) sum to give the first term on the righthand side in Fig. 7.

The last graph in Fig. 4 is

$$\int_0^1 d^0 \int_0^1 \frac{d^0}{2} \int_0^1 \frac{d^4 q}{(2)^4} \int_0^1 \frac{d^4 q^0}{(2)^4} \frac{1}{i''} \int_0^1 (q; q) D(q) S_F(q) \int_0^1 (q; q); \quad (79)$$

Using the approximation (72), the integrand in (79) becomes

$$\int_0^1 d^0 \int_0^1 \frac{d^0}{2} \int_0^1 \frac{d^4 q^0}{(2)^4} \frac{1}{i''} \int_0^1 (q^0; p_2; q^0; q^0) \int_0^1 D(q) S_F(q) \int_0^1 (q^0; p_1; q^0; q^0) S_F(q^0) \int_0^1 (q^0; q^0); \quad (80)$$

plus a similar term in which the gluon couples leg  $p_2$  to  $p_3$ . Other terms are either ignored because they only correct the external legs or else not distinct because of the symmetries of the amplitude. The term given in (80) may be summed with the second graph on the righthand side of the equation in Fig. 4 to give

$$\int_0^1 d^0 \int_0^1 \frac{d^0}{2} \int_0^1 \frac{d^4 q}{(2)^4} \int_0^1 \frac{d^4 q^0}{(2)^4} V_{q; p_2; q^0; p_1} (q; q) \frac{S_F(q) S_F(q)}{i''} \int_0^1 (p_3; q^0; p_4; q^0) \int_0^1 (q; q); \quad (81)$$

This is the second graph on the righthand side in Fig. 7. The remaining graphs in Fig. 7 result from (81) by complex conjugation (reversing the spurion line) and by the substitution  $p \rightarrow p$ . We have, finally,

$$\begin{aligned} V_{p_3; p_2; p_4; p_1} (q; q) = & V_{p_3; p_2; p_4; p_1} (q; q) + \int_0^1 d^0 \int_0^1 \frac{d^0}{2} \int_0^1 \frac{d^4 q}{(2)^4} \int_0^1 \frac{d^4 q^0}{(2)^4} \\ & \left( V_{q; p_2; q^0; p_1} (q; q) \frac{S_F(q) S_F(q)}{i''} \int_0^1 (p_3; q^0; p_4; q^0) \int_0^1 (q; q) \right. \\ & + V_{q; p_2; q^0; p_1} (q; q) \frac{S_F(q) S_F(q)}{i''} V_{p_3; q^0; p_4; q^0} (q; q) \\ & + V_{q^0; p_4; p_1} (q; q) \frac{S_F(q) S_F(q^0)}{i''} \int_0^1 (p_3; p_2; q^0; q^0) \int_0^1 (q; q) \\ & \left. + V_{q^0; p_4; p_1} (q; q) \frac{S_F(q) S_F(q^0)}{i''} V_{p_3; p_2; q^0; q^0} (q; q) \right); \end{aligned} \quad (82)$$

It would be interesting to approximate  $V$  further by just taking the long range (small  $q$ ) part calculated in Sec. IIID and substituting this in (82). The divergence in  $V$  will be cancelled by divergences in the self-energy corrections to the external legs (see Sec. IIID) — corrections which we have ignored here but which must be included if one wants to solve this Bethe-Salpeter-like equation in a consistent manner. This paper is long enough already, and therefore such a calculation will not be undertaken here.

## V. CLOSING ARGUMENTS

In this paper we have developed a similarity renormalization framework for the study of strongly interacting field theories. The basic view of this approach is that Hamiltonian methods will prove most fruitful for the solution of such theories. The generic theory for which our framework has been developed has interactions that are weak asymptotically but grow large enough at low energy to invalidate perturbation theory. QCD is of course the theory that we particularly have in mind. The basic idea behind the similarity renormalization scheme is that the Hamiltonian of such a theory can be transformed into that of an effective many-body theory where states that differ greatly in free energy are essentially uncoupled. This resulting many-body Hamiltonian can then be solved with recourse to the many available approximate methods such as variational approaches, trial wave functions, iterative techniques and numerical basis function approaches. The similarity transformation achieves this goal by smoothly eliminating interactions between states whose free energies differ by an amount greater than an arbitrary scale introduced by the transformation. The result of this elimination is to create new interactions between states that differ in energy by an amount less than  $\Lambda$ . The assumption is that from these new interactions one can extract potentials that describe the relevant physics.

Clearly, no physical result can depend on the renormalization scale  $\Lambda$ . However, the calculations can only be approximately carried out for most systems of interest, and so one will need to choose a value of  $\Lambda$  that makes the approximations as valid as possible. Computations in this framework involve two steps: first, the similarity transformed Hamiltonian is calculated; second, this Hamiltonian is solved. The first step is most easily done perturbatively, which requires that  $\Lambda$  be large since only at high energy is the coupling small (by assumption). The second step is most easily done when as few states as possible are coupled strongly, which requires that  $\Lambda$  be as small as possible. Inevitably, one must make a compromise and choose  $\Lambda$  in some intermediate range. If the Dyson-Schwinger-like equations developed in the last section can be implemented, it may be possible to go beyond the perturbative calculation of the dressed Hamiltonian so that  $\Lambda$  can be lowered to values for which perturbation theory begins to break down. However, in most cases it will probably be better to keep  $\Lambda$  large enough that the Hamiltonian can be dressed perturbatively, since the tools available for the second step are generally more powerful.

That the elimination of couplings between states separated by large energy differences turns a field theory into a many-body theory is clear if the free particles are massive. If  $\Lambda$  is lowered to just above the particle masses, then creating or destroying a particle will cause an energy difference of order  $\Lambda$ . This means interactions that change particle number will be suppressed. If the particles are light or massless, however, as in QCD, it does not follow that the similarity transformation described here will suppress interactions that change particle number. Indeed, one might consider it better to have the similarity function depend on differences in particle number rather than on differences in energy. However, such a transformation is unlikely to be feasible in perturbation theory, for one no longer has a means of eliminating only high energy degrees of freedom. Moreover, one would lose the advantage that small energy denominators are avoided. Instead, one can use the similarity transformation in a light-front formulation of a theory such as QCD. We shall argue in the following that this change of formulation of the theory will provide a means of turning even



QCD into a many-body problem.

The use of light-front coordinates in field theory is not new (see Ref. [3] for a review and an exhausting — if perhaps not quite exhaustive — list of references). Such calculations are considered difficult, partly because they are unfamiliar, but also because they really are difficult. One of the major difficulties with the use of light-front coordinates is that Lorentz covariance is no longer manifest once one chooses a particular direction in defining the light-front time. Another problem is that calculations are only feasible for a particular gauge choice, the light-cone gauge. These problems severely complicate the renormalization of divergences, and this has slowed advance in light-front computations. The fact that in our similarity renormalization scheme the calculation of the dressed Hamiltonian can be expressed in terms of Feynman diagrams is therefore significant. It means that divergences can be handled with dimensional regularization, the infrared singularities can be handled with the Mandelstam-Leibbrandt prescription, and the counterterm structure is then that of covariant formulations. In particular, renormalization of divergences for QCD in equal-time coordinates and the light-cone gauge is well understood (see, for example, Refs. [10–11]), and we can rely on such prior work in determining the dressed Hamiltonian in the intermediate representation. There are of course other, more technical difficulties resulting from the choice of light-front coordinates (for example, rotations about the transverse axes are no longer kinematical); but these should not be prohibitive. Indeed, there are also some technical advantages to the use of light-front as compared to equal-time coordinates (for example, now boosts are kinematical).

The essential reasons for using light-front coordinates follow from the free particle dispersion relation

$$p^- = \frac{p_\perp^2 + m^2}{p^+} : \quad (83)$$

This implies that all on-shell particles (and antiparticles) have longitudinal momentum  $p^+ > 0$  and all physical states have total longitudinal momentum  $P^+ > 0$ . The vacuum has  $P^+ = 0$  and is therefore built only from particles with  $p^+ = 0$ . From (83) we see that such particles have infinite (light-front) energy unless  $p_\perp^2 = 0$  and  $m^2 = 0$ . The similarity transformation will decouple the infinite energy states from the low-energy physics, and the computation of the vacuum state is then greatly simplified. Indeed, if we give gluons a small mass, all particles with  $p^+ = 0$  have infinite energy, and the vacuum state of the dressed Hamiltonian is just the trivial free vacuum state. Likewise, in building any bound state of the dressed Hamiltonian, we can rely on the fact that the total longitudinal momentum  $P^+$  must be built up from constituent longitudinal momenta  $p_i^+ > 0$ . If the energy of each constituent is to be less than  $E$ , we must have  $p_i^+ \geq (p_\perp^2 + m^2)/E$  for all  $p_i^+$ , and thus in effect we have a bound on the number of particles that can make up a state. Again, the only particles that escape this lower bound on the longitudinal momentum are (massless) gluons with  $p_\perp^2 = 0$ , but one can hope that such highly transversely localized particles will have little contribution to low-energy states. In any case, it is clear that effects associated with the quark-gluon sea in the equal-time formulation of QCD will be largely, if not totally, replaced by interactions in the dressed Hamiltonian after a similarity transformation in the light-front formulation.

But the most interesting result of the light-front formulation is that longitudinal and transverse variables scale differently (this has been repeatedly emphasized by Wilson<sup>17</sup>).

This can be seen from the dispersion relation (83) and has been discussed in Sec. III D. Thus the similarity renormalization of light-front Hamiltonians depends on the energy scale through both a mass scale and a longitudinal momentum scale. The mass scale may be taken to be that introduced by dimensional regularization. The QCD coupling  $g_R$  runs with this scale, and  $\mu$  must be taken large to keep  $g_R$  small enough for perturbation theory to remain valid. However, the similarity function  $f$  runs with the ratio  $\mu^2 = \Lambda^2$ ; and thus, even though the mass scale be large, we can suppress couplings between states with energy differences above a given value by making the longitudinal scale large enough. We have seen that light-front energy increases with particle number; and therefore at large the similarity transformation will suppress number changing interactions in the dressed Hamiltonian, thus turning the solution of QCD bound states into a many-body problem. That the mass scale may be nevertheless kept large provides the possibility that the transformation may be accurately calculated in perturbation theory. That Dyson's intermediate representation is a particular similarity renormalization scheme that may be expressed in terms of ordinary Feynman graphs means that perturbative light-front QCD computations are feasible. These computations should yield a dressed Hamiltonian that is considerably closer to strong-interaction phenomenology than the usual free QCD Hamiltonian. That we find a confining potential already at tree level may be taken as a positive indication of the utility of this approach.

#### Acknowledgements

I have benefited from past discussions with Ken Wilson, Avaroth Harindrinath and Robert Perry. I thank J.S. Walhout for first pointing out Ref.[6] to me.

## REFERENCES

- <sup>1</sup> K.G. Wilson, Phys. Rev. 140, B445 (1965).
- <sup>2</sup> St.D. Glazek and K.G. Wilson, Phys. Rev. D 48, 5863 (1993), D 49, 4214 (1994).
- <sup>3</sup> K.G. Wilson, T.S. Walhout, A. Harindranath, W.M. Zhang, R.J. Perry and St.D. Glazek, Phys. Rev. D 49, 6720 (1994).
- <sup>4</sup> K. Wegner, Ann. Physik 3, 77 (1994).
- <sup>5</sup> F.J. Dyson, Phys. Rev. 82, 428 (1951); 83, 608 (1951); 83, 1207 (1951); and Proc. Roy. Soc. London A 207, 395 (1951).
- <sup>6</sup> For a brief historical account of Dyson's papers, see S.S. Schweber, QED and the Men Who Made It: Dyson, Feynman, Schwinger, and Tomonaga, (Princeton University Press, Princeton, 1994) pp. 556-565.
- <sup>7</sup> V.G. Kadashevsky, Sov. Phys. JETP 19, 443, 597 (1964); Nuc. Phys. 6, 125 (1968).
- <sup>8</sup> For a review, with emphasis on a light-front formulation, see V.A. Karamov, Sov. J. Part. Nucl. 19, 228 (1988).
- <sup>9</sup> W.M. Zhang and A. Harindranath, Phys. Rev. D 48, 4881 (1993).
- <sup>10</sup> A. Bassetto, M. D'Albaso and R. Soldati, Phys. Rev. D 36 (1987) 3138.
- <sup>11</sup> A. Bassetto, G. Nardelli and R. Soldati, Yang-Mills Theories in Algebraic Non-Covariant Gauges (World Scientific, Singapore, 1991).
- <sup>12</sup> H.C. Lee and M.S. Milgram, Nuc. Phys. B 268, 543 (1986).
- <sup>13</sup> R.J. Perry, in Hadron Physics 94, ed. by V.E. Herscovitz and C. Vasconcellos (World Scientific, Singapore, 1995); and in Theory of Hadrons and Light-Front QCD, ed. by St.D. Glazek (World Scientific, Singapore, 1994) pp. 56-70.
- <sup>14</sup> W.M. Zhang, Phys. Rev. D 56, 1528 (1997).
- <sup>15</sup> K.G. Wilson and D.R. Robertson, in Theory of Hadrons and Light-Front QCD, ed. by St.D. Glazek (World Scientific, Singapore, 1994) pp. 15-28.
- <sup>16</sup> S. Mandelstam, Nucl. Phys. B 213, 718 (1983); G. Leibbrandt, Phys. Rev. D 29, 1699 (1984).
- <sup>17</sup> K.G. Wilson, OSU internal reports, 1989, 1990, 1993 (unpublished); and private communication.

# FIGURES

FIG .1. Doubled Feynman graph

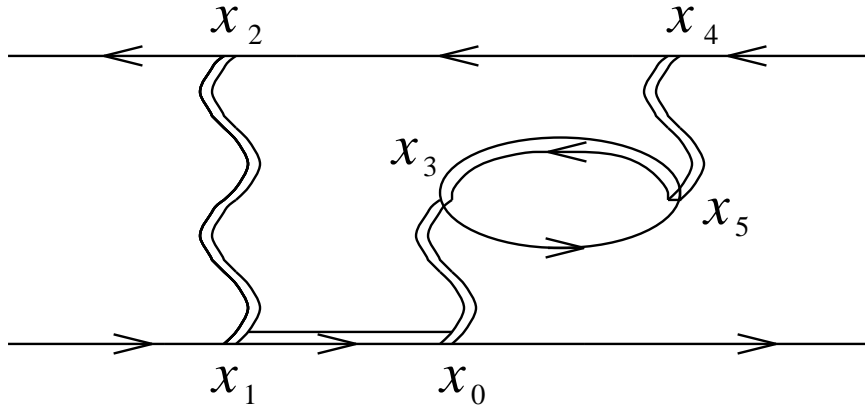


FIG .2. Spurion graph corresponding to Figure 1

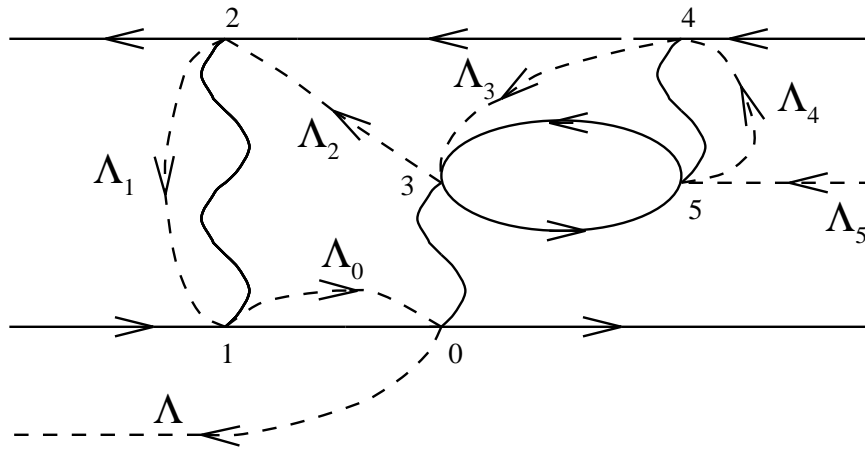
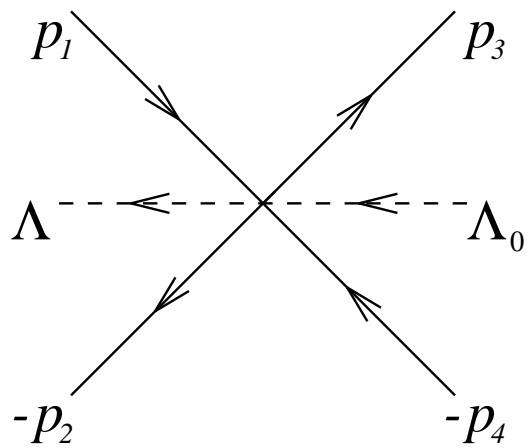
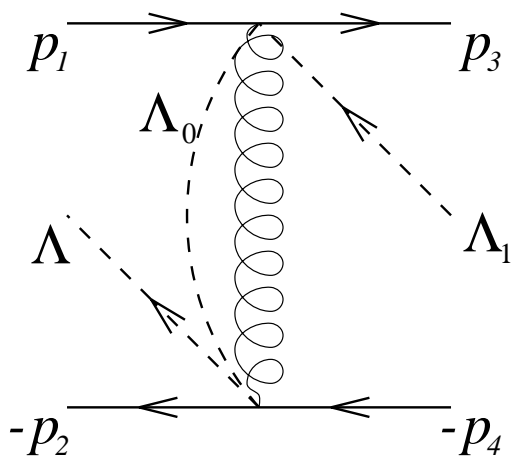


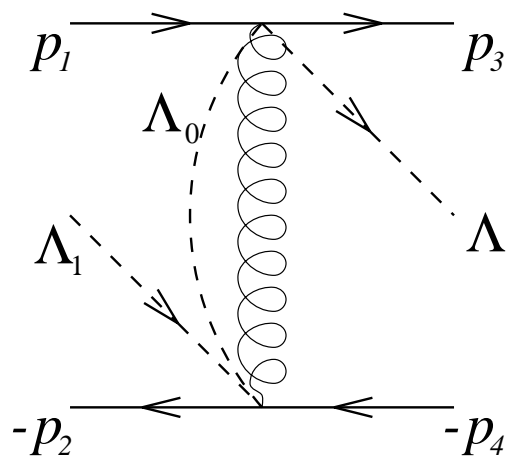
FIG. 3. Order  $g_R^2$  diagrams contributing to  $qq \rightarrow qq$



(a)



(b)



(c)

FIG .4. Diagrammatic equation for general  $qq \rightarrow qq$  vertex

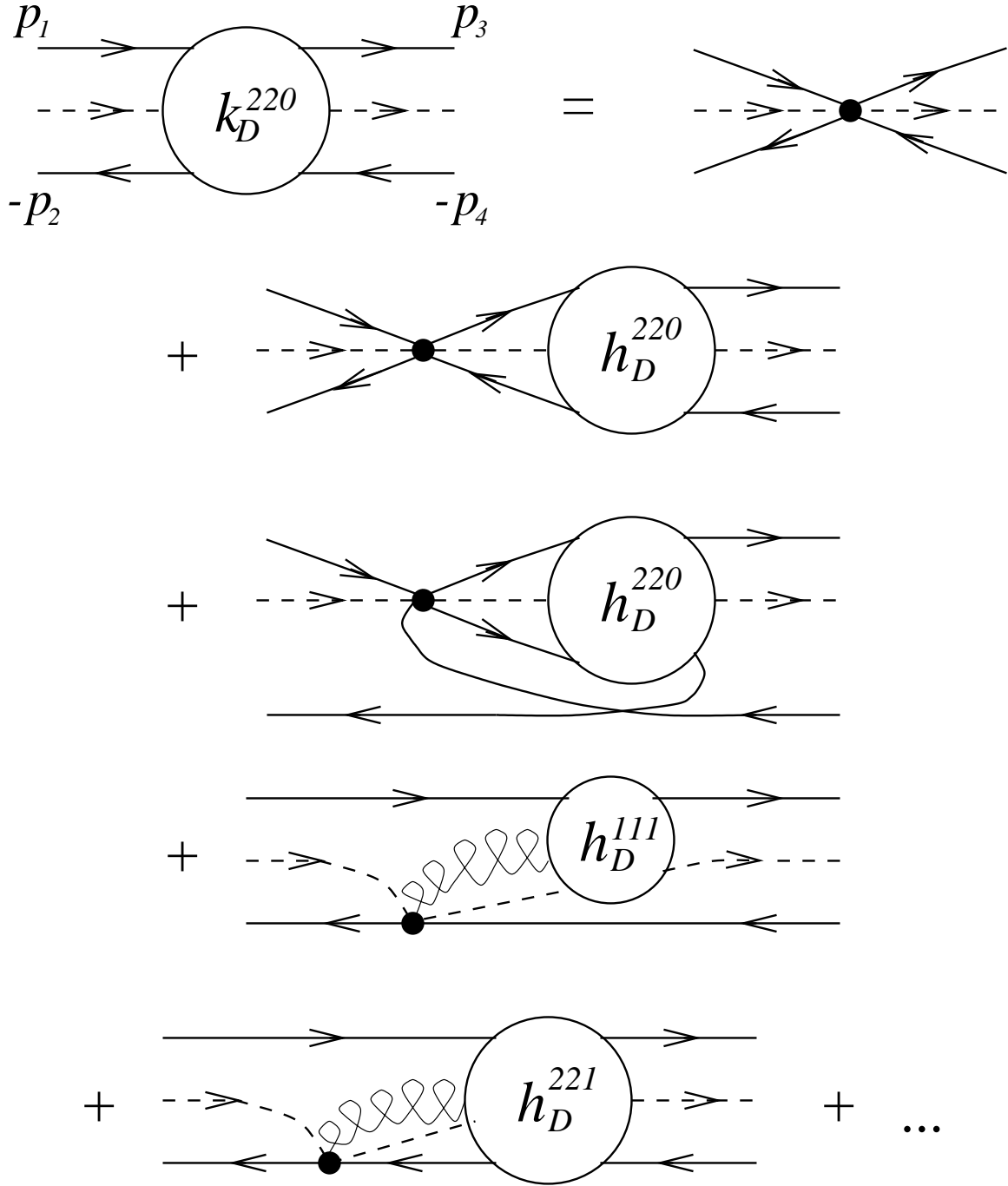


FIG. 5. Approximations for  $q \rightarrow qg$  and  $q\bar{q}g \rightarrow q\bar{q}$  vertices

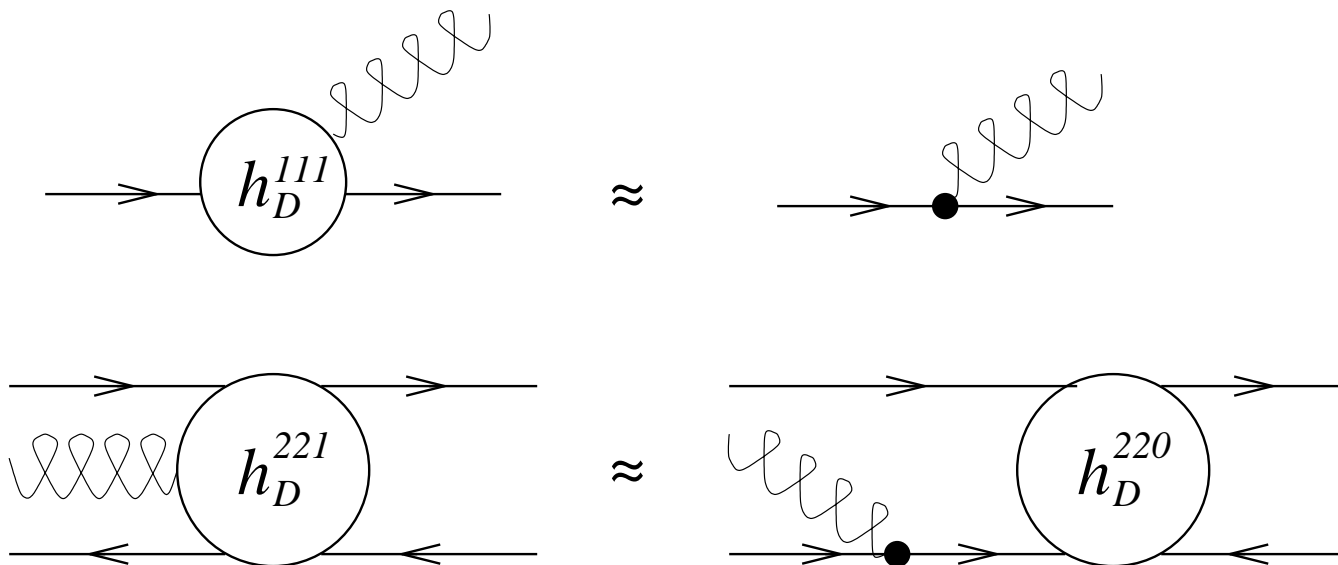


FIG. 6. Definition of input potential for approximation to  $q\bar{q} \rightarrow q\bar{q}$  vertex

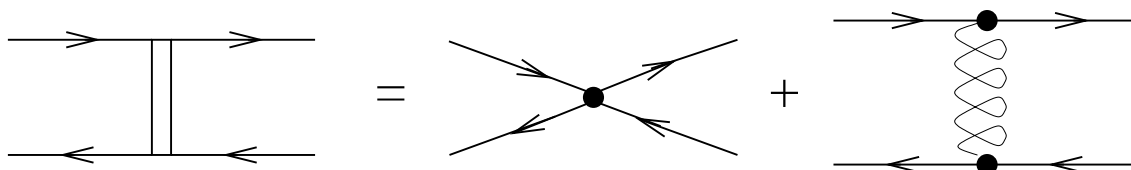


FIG .7. Bethe-Salpeter-like approximation to  $q\bar{q} \rightarrow q\bar{q}$  vertex

